4. R. D. Vale *et al.*, *Nature* **380**, 451 (1996).
5. H. Noji, R. Yasuda, M. Yoshida, K. Kinosita, *Nature* **386**, 299 (1997).
6. M. D. Wang *et al.*, *Science* **282**, 902 (1998).
7. H. P. Lu, L. Y. Xun, X. S. Xie, *Science* **282**, 1877 (1998).
8. M. Rief, M. Gautel, F. Oesterhelt, J. M. Fernandez, H. E. Gaub, *Science* **276**, 1109 (1997).
9. M. S. Z. Kellermayer, S. B. Smith, H. L. Granzier, C. Bustamante, *Science* **276**, 1112 (1997).
10. L. Tskhovrebova, J. Trinick, J. A. Sleep, R. M. Simmons, *Nature* **387**, 308 (1997).
11. R. M. Dickson, A. B. Cubitt, R. Y. Tsien, W. E. Moerner, *Nature* **388**, 355 (1997).
12. R. F. Gesteland and J. F. Atkins, Eds., *The RNA World* (Cold Spring Harbor Laboratory Press, Cold Spring Harbor, NY, 1993).
13. D. W. Celander and T. R. Cech, *Science* **251**, 401 (1991).
14. P. P. Zarrinkar and J. R. Williamson, *Science* **265**, 918 (1994).
15. B. Sclavi, M. Sullivan, M. R. Chance, M. Brenowitz, S. A. Woodson, *Science* **279**, 1940 (1998).
16. J. Pan, D. Thirumalai, S. A. Woodson, *J. Mol. Biol.* **273**, 7 (1997).
17. D. K. Treiber, M. S. Rook, P. P. Zarrinkar, J. R. Williamson, *Science* **279**, 1943 (1998).
18. R. Russell and D. Herschlag, *J. Mol. Biol.* **291**, 1155 (1999).
19. T. Pan, *Biochemistry* **34**, 902 (1995).
20. P. P. Zarrinkar, J. Wang, J. R. Williamson, *RNA* **2**, 564 (1996).
21. X. Fang, T. Pan, T. R. Sosnick, *Nature Struct. Biol.* **6**, 1091 (1999).
22. T. R. Cech and D. Herschlag, *Nucleic Acids Mol. Biol.* **10**, 1 (1996).
23. Supplementary material is available at www.sciencemag.org/feature/data/1049406.shl.
24. To assess the specificity of ribozyme binding, streptavidin-coated surfaces were incubated with ribozyme bound to biotinylated and non-biotinylated tethers. The former gave 100-fold greater surface density of fluorescently labeled molecules than the latter, demonstrating that the biotinylated ribozyme binds to the surface predominately through the biotin-streptavidin interaction.
25. In the total internal reflection microscope, fluorescent molecules were excited by an evanescent wave generated by total internal reflection of a 514-nm laser beam and detected by a CCD (charge-coupled device) camera (*23*). The microscope could detect several hundred individual molecules simultaneously with a time resolution of 100 ms. The cleavage kinetics and overall folding kinetics were measured using this apparatus. In the scanning confocal microscope, fluorescent molecules were excited by a focused 514-nm laser beam and detected by avalanche photodiodes. This apparatus can measure the fluorescence emission of one molecule with a time resolution of 1 ms. The docking kinetics were measured using this apparatus.
26. D. Herschlag and T. R. Cech, *Biochemistry* **29**, 10159 (1990).
27. Bulk measurements were carried out by the conventional single-turnover radioactive assay (*26*). Ribozyme (100 nM) was bound to a trace amount (<1 nM) of 5′-[^{32}P]-labeled S. After ≥1 min for binding of S, cleavage was initiated by addition of G. Reactions measuring the rate constant for S binding were carried out as previously described (*26*).
28. The identical k_{max} indicate that the ternary complex of ribozyme·S·G is unperturbed by the surface. Under the conditions used in the experiments, $K_{1/2}^{G}$ is equal to K_d^{G}, the equilibrium dissociation constant of G [T. S. McConnell, T. R. Cech, D. Hershlag, *Proc. Natl. Acad. Sci. U.S.A.* **90**, 8362 (1993)]; thus, the identical $K_{1/2}^{G}$ indicates that the G binding site is unperturbed by the surface.
29. L. Stryer and R. P. Haugland, *Proc. Natl. Acad. Sci. U.S.A.* **58**, 719 (1967).
30. G. J. Schutz, W. Trabesinger, T. Schmidt, *Biophys. J.* **74**, 2223 (1998).
31. T. Ha *et al.*, *Proc. Natl. Acad. Sci. U.S.A.* **96**, 893 (1999).
32. T. Ha *et al.*, *Proc. Natl. Acad. Sci. U.S.A.* **96**, 9077 (1999).
33. The FRET efficiency is given by $1/[1 + (R/R_0)^6]$, where R is the distance between the donor and acceptor. R_0 is typically between 3 and 7 nm, depending on the spectral overlap between the donor emission and acceptor absorption, quantum yield of the donor, and the orientations of the donor and acceptor. Thus, the FRET efficiency strongly depends on the distance between donor and acceptor as well as their orientations. Although there is a strong expectation of a large decrease in distance between the donor and acceptor upon P1 docking or overall folding, the conclusions here are independent of whether the FRET efficiency responds to changes in distance, orientation, or both.
34. D. Herschlag, *Biochemistry* **31**, 1386 (1992).
35. P.C. Bevilacqua, R. Kierzek, K. A. Johnson, D. H. Turner, *Science* **258**, 1355 (1992).
36. J. A. Latham and T. R. Cech, *Science* **245**, 276 (1989).
37. B. L. Golden, A. R. Gooding, E. R. Podell, T. R. Cech, *Science* **282**, 259 (1998).
38. V. Lehnert, L. Jaeger, F. Michel, E. Westhof, *Chem. Biol.* **3**, 993 (1996).
39. J.-F. Wang, W. D. Downs, T. R. Cech, *Science* **260**, 504 (1993).
40. G. J. Narlikar and D. Herschlag, *Nature Struct. Biol.* **3**, 701 (1996).
41. Previous studies of the rate constants for docking (*35*, *45*), using different substrates under different conditions, yielded values within the same order of magnitude as reported here.
42. A. R. Fersht, A. Matouschek, L. Serrano, *J. Mol. Biol.* **244**, 771 (1992).
43. A. M. Pyle, F. L. Murphy, T. R. Cech, *Nature* **358**, 123 (1992).
44. D. Herschlag, F. Eckstein, T. R. Cech, *Biochemistry* **32**, 8299 (1993).
45. G. J. Narlikar, L. E. Bartley, M. Khosla, D. Herschlag, *Biochemistry* **38**, 14192 (1999).
46. R. Russell and D. Herschlag, unpublished data.
47. J. Pan and S. Woodson, *J. Mol. Biol.* **280**, 597 (1998).
48. To demonstrate that the ribozyme attains its native state when the FRET value reaches ≥0.8, ribozyme molecules were unfolded with a buffer lacking Mg^{2+} and refolded with a buffer containing 5 mM Mg^{2+} and 0.3 mM G. The time traces with FRET reaching ≥0.8 after refolding show simultaneous disappearance of both donor and acceptor signals within a few seconds, due to the cleavage of S. The histogram of the time between FRET reaching ≥0.8 and disappearance of fluorescence shows a single exponential decay with a rate constant of 0.25 s^{-1}, the same as the cleavage rate constant obtained from prefolded ribozyme.

49. We are grateful to S. A. Scaringe and J. A. Orr for their advice on oligonucleotide preparation. This research was supported by an NSF grant (PHY-9970017) and an Air Force Office of Scientific Research grant (F49620-98-1-0219) to S.C. and an NIH grant (GM49423) to D.H. X.Z. was supported by the Chodorow Fellowship of the Stanford Applied Physics Department and an NIH postdoctoral fellowship. L.E.B. was supported in part by an NIH training grant. H.P.B. was supported in part by a Center on Polymer Interfaces and Macromolecular Assemblies grant. R.R. was supported by an NIH postdoctoral fellowship.

11 February 2000; accepted 28 April 2000

Role of CD47 as a Marker of Self on Red Blood Cells

Per-Arne Oldenborg,[1] Alex Zheleznyak,[1] Yi-Fu Fang,[1] Carl F. Lagenaur,[2] Hattie D. Gresham,[3] Frederik P. Lindberg[1]*

The immune system recognizes invaders as foreign because they express determinants that are absent on host cells or because they lack "markers of self" that are normally present. Here we show that CD47 (integrin-associated protein) functions as a marker of self on murine red blood cells. Red blood cells that lacked CD47 were rapidly cleared from the bloodstream by splenic red pulp macrophages. CD47 on normal red blood cells prevented this elimination by binding to the inhibitory receptor signal regulatory protein alpha (SIRPα). Thus, macrophages may use a number of nonspecific activating receptors and rely on the presence or absence of CD47 to distinguish self from foreign. CD47-SIRPα may represent a potential pathway for the control of hemolytic anemia.

Natural killer (NK) cells eliminate target cells recognized by a range of activating receptors that bind ligands on many normal cells. However, expression of self major histocompatibility complex (MHC) class I molecules can protect a cell by binding to NK cell inhibitory receptors, which recruit and activate *src*-homology phosphatases (SHP-1 and SHP-2) that inhibit cell activation (*1*–*4*). NK cells thus spare cells that express "markers of normal self" in the form of MHC class I molecules, and eliminate them when these markers are absent or inadequately expressed. In contrast to what might be expected, MHC class I–deficient mice are not autodestructive. Rather, NK cell recognition adapts to the level of inhibitory ligand expressed in the NK cell environment (*5*). Expression of molecules related to NK cell inhibitory receptors on other leukocytes suggests that similar mechanisms are operative, for example, in macrophage activation (*4*, *6*, *7*). Although many of these molecules recognize MHC class I, the "marker of self" could in principle be any ubiquitously expressed surface molecule.

[1]Division of Infectious Diseases, Department of Internal Medicine, Campus Box 8051, Washington University School of Medicine, 660 South Euclid Avenue, St. Louis, MO 63110, USA. [2]Department of Neurobiology, School of Medicine, University of Pittsburgh, Pittsburgh, PA 15261, USA. [3]Research Service, Albuquerque VA Medical Center, Albuquerque, NM 87108, USA.

*To whom correspondence should be addressed. E-mail: lindberg@id.wustl.edu

SIRPα is a unique receptor in that it appears to bind CD47 (integrin-associated protein, IAP), a ubiquitously expressed cell surface glycoprotein, rather than MHC (*8–14*). SIRPα is expressed on many cells, most abundantly on polymorphonuclear leukocytes, monocytes, and monocyte-derived cells, where it is an inhibitory receptor (*8–14*). In contrast to MHC, CD47 is present also on red blood cells (RBCs). We hypothesized that CD47 might function as a RBC marker of self, and that CD47-deficient cells would therefore be rapidly destroyed by SIRPα−expressing leukocytes.

$CD47^{-/-}$ mice are viable and have normal RBC parameters (*15*, *16*). To investigate whether $CD47^{-/-}$ RBCs can survive in wild-type mice, we transfused $CD47^{-/-}$ and control recipients with $CD47^{-/-}$ and wild-type ($CD47^{+}$) RBCs (*17*). Transfused $CD47^{-/-}$ RBCs were rapidly eliminated from the circulation of wild-type recipients, but were not affected in $CD47^{-/-}$ recipients (Fig. 1A). Wild-type RBCs were unaffected in both recipient types (Fig. 1B). Elimination of the $CD47^{-/-}$ RBCs was not due to recognition of the *null* allele itself, but rather due to recognition of the CD47-deficient state, because heterozygotes were indistinguishable from the wild-type both as donors and as recipients. Antibody and classical T and B cells were not required for the elimination of RBCs, because clearance was rapid also in immune- and antibody-deficient $Rag1^{-/-}$ mice (Fig. 1C). Furthermore, gene-targeted mice deficient in complement component 3 (C3) were similarly able to eliminate $CD47^{-/-}$ RBCs, suggesting that complement activation was not required (Fig. 1D).

Clearance of RBCs occurs primarily in the spleen. To determine if this was the case for the rapid elimination of $CD47^{-/-}$ RBCs, we compared elimination of $CD47^{-/-}$ RBCs in splenectomized or sham-operated wild-type recipients to that in unoperated wild-type and $CD47^{-/-}$ controls (Fig. 2A). Elimination of $CD47^{-/-}$ RBCs was almost completely abolished by splenectomy, whereas sham operation had no effect. Thus, the spleen was required for the elimination of $CD47^{-/-}$ RBCs.

Dichloromethylene diphosphonate (clodronate)–loaded liposomes injected intravenously kill splenic macrophages (*18*). Different repopulation kinetics make it possible to determine the relative contribution of various splenic macrophage subsets to a phenotype (*19*). Treatment of wild-type mice with clodronate liposomes (*20*) prevented the elimination of $CD47^{-/-}$ RBCs, strongly suggesting that clearance was effected by macrophages (Fig. 2B). Recovery was already substantial 10 days after clodronate injection and virtually complete at day 28. This is consistent with the repopulation kinetics of red pulp macrophages, but not with those of marginal metallophilic macrophages (about 3 weeks) and marginal zone macrophages (about 2 months) (*20*). Thus, splenic macrophages were required for $CD47^{-/-}$ RBC elimination, and among them, red pulp macrophages were sufficient. The identification of red pulp macrophages as the primary site of $CD47^{-/-}$ RBC clearance was confirmed by immunohistochemistry (*21*) (Fig. 3) and by flow cytometry.

SIRPα, a receptor for CD47, is thought to generate macrophage-inhibitory signals (*8*, *22*, *23*). It is highly expressed on myeloid cells, including red pulp macrophages (*22–24*). If SIRPα is the relevant receptor for RBC clearance, antibodies to SIRPα (anti-SIRPα) that block SIRPα-CD47 interaction should augment the phagocytosis of wild-type RBCs to the same extent as that seen with $CD47^{-/-}$ targets. Indeed, isolated splenic macrophages (mainly $F4/80^{+}$ red pulp

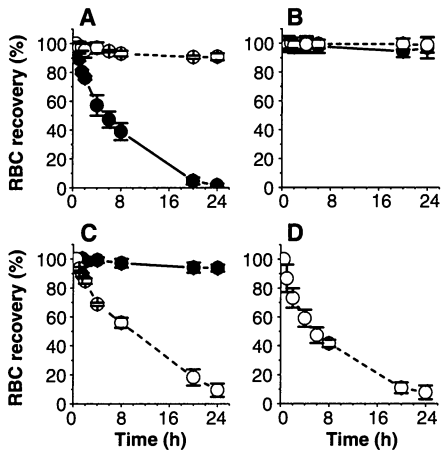

Fig. 1. Wild-type mice rapidly eliminate CD47-deficient RBCs independently of antibody and complement. Fluorescently labeled RBCs were injected intravenously. At the times indicated, 5 μl of venous blood was sampled from a tail vein of the recipients and analyzed by flow cytometry for the fraction of fluorescent RBCs (*17*). Data were normalized to the level at 30 min after injection (usually 4 to 6% of total RBCs). (**A**) $CD47^{-/-}$ RBCs were injected into wild-type (●) or $CD47^{-/-}$ (○) recipients. (**B**) Wild-type RBCs were injected into wild-type (●) or $CD47^{-/-}$ (○) recipients. (**C**) Wild-type RBCs (●) or $CD47^{-/-}$ RBCs (○) were injected into CD47 wild-type $rag1^{-/-}$ recipients. (**D**) $CD47^{-/-}$ RBCs were injected into CD47 wild-type $C3^{-/-}$ recipients. Data are the means ± SD for three to four recipients per group.

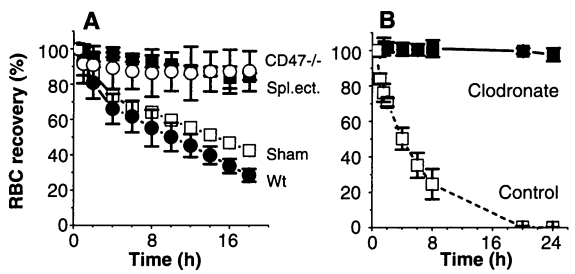

Fig. 2. Clodronate-sensitive cells in the spleen of wild-type mice are necessary for the clearance of $CD47^{-/-}$ RBCs. (**A**) Lack of clearance of $CD47^{-/-}$ RBCs in splenectomized wild-type recipients. Wild-type mice were splenectomized (■) or sham-operated (□). Fourteen days later, the clearance of $CD47^{-/-}$ RBCs in these mice was compared with that in unoperated wild-type and $CD47^{-/-}$ recipients (*17*). For comparison, the clearance in wild-type (●) or $CD47^{-/-}$ (○) recipients is shown. Data are the means ± SD for one to three recipients per group. (**B**) Elimination of clodronate-sensitive cells abolishes the clearance of $CD47^{-/-}$ RBCs in wild-type recipients. Wild-type mice were injected intravenously with clodronate liposomes (■) or, as a control, liposomes prepared without clodronate (□) (*20*) at 48 and 24 hours before the examination of $CD47^{-/-}$ RBC clearance (*17*). Data are the means ± SD for five clodronate-treated mice and four mice treated with control liposomes.

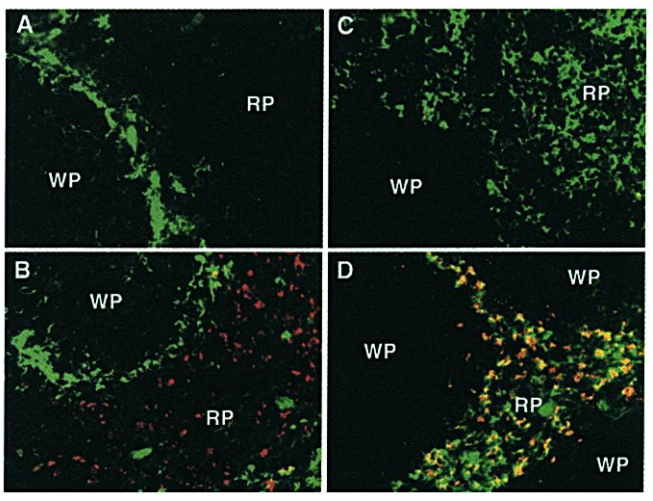

Fig. 3. Splenic $F4/80^{+}$ red pulp macrophages are responsible for clearance of $CD47^{-/-}$ RBCs in wild-type mice. $CD47^{-/-}$ (**A** and **C**) or wild-type (**B** and **D**) recipients were injected with fluorescent red (PKH26) $CD47^{-/-}$ RBCs, and spleens were harvested 20 hours later. Frozen spleen sections were stained green for either MOMA-1 (a marker for marginal metallophilic macrophages) (A and B) or F4/80 (a marker for red pulp macrophages) (C and D) (*21*). RP, red pulp; WP, white pulp.

macrophages) in vitro phagocytosed CD47$^{-/-}$ RBCs at a high rate, whereas wild-type RBCs remained almost completely unaffected (*24*) (Fig. 4A). Antibody P84 is directed against SIRPα and blocks CD47-SIRPα interaction (*9*). This antibody had no effect on the phagocytosis of CD47$^{-/-}$ RBCs, but increased phagocytosis of wild-type RBCs to the same extent as that seen with CD47$^{-/-}$ targets (Fig. 4A). Thus, inhibition of phagocytosis by CD47 on the target RBCs required SIRPα and SIRPα-CD47 interaction. The observation that both types of RBCs were phagocytosed equivalently when SIRPα was blocked strongly suggests that CD47$^{-/-}$ RBCs are cleared because of the absence of CD47 on their surface, rather than because of a possible secondary effect of CD47 deficiency on the RBCs.

SIRPα contains intracellular immune receptor tyrosine-based inhibitory motifs, which

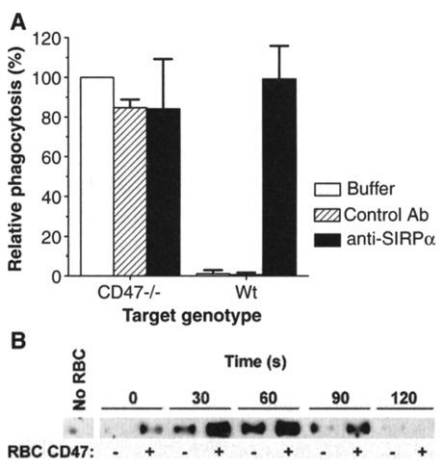

Fig. 4. CD47 on RBCs inhibits phagocytosis through binding to macrophage SIRPα. (**A**) Adherent wild-type splenic macrophages were incubated without antibody (open bars), with 5 μg of anti-SIRPα mAb P84 (*9*) (closed bars), or with 5 μg of the isotype-matched anti-murine CD14 control antibody (rmC5-3) (hatched bars) for 15 min before the addition of wild-type or CD47$^{-/-}$ RBCs (*24*). After lysis of noningested RBCs, the number of ingested RBCs per 100 macrophages was determined under each condition. Data shown are normalized to the level of phagocytosis of CD47$^{-/-}$ RBCs in the absence of antibody (63 ± 15 RBCs per 100 macrophages). Data are the means ± SD for three separate experiments. (**B**) Macrophage SIRPα1 tyrosine phosphorylation upon contact with CD47 on RBCs. RBCs were allowed to sediment onto bone marrow–derived macrophages in ice-cold buffer. Cells were then rapidly warmed to 37°C in the presence of 2 mM pervanadate and lysed in sample buffer at the times indicated. Anti-SIRPα mab P84 immunoprecipitates were separated by SDS-PAGE and analyzed by Western blot for phosphotyrosine with mAb 4G10 and by using enhanced chemoluminescence (*27*). Phosphorylation is more pronounced and occurs earlier in contact with wild-type RBCs than with CD47$^{-/-}$ RBCs, indicating that CD47 on the target induces a SIRPα signal.

upon binding and aggregation are phosphorylated by *src*-family kinases, leading to the recruitment and activation of tyrosine phosphatases SHP-1 and/or SHP-2 (mainly SHP-1 in macrophages) (*25*). This in turn inhibits signaling in tyrosine kinase–dependent activation pathways (*8*, *26*). In contrast to splenic macrophages, bone marrow–derived macrophages (BMMs) do not phagocytose CD47$^{-/-}$ RBCs, allowing study of the inhibitory signal in isolation. To investigate whether CD47 on RBCs could induce a macrophage SIRPα signal, we assayed SIRPα tyrosine phosphorylation (*8*, *27*) in BMMs after contact with either CD47$^{-/-}$ or wild-type RBCs. Wild-type RBCs induced markedly greater SIRPα tyrosine phosphorylation than CD47$^{-/-}$ RBCs (Fig. 4B). The increase in SIRPα phosphorylation in the presence of CD47$^{-/-}$ RBCs was similar to that seen without RBCs and was probably due to interactions between macrophage CD47 and SIRPα or to the temperature shift in the experiment. Thus, RBC CD47 can induce a macrophage SIRPα signal.

Because CD47 binds SIRPα, regulation of CD47 expression might serve as a mechanism to control elimination or uptake of damaged or senescent RBCs. However, RBC CD47 expression is very narrowly distributed, with a negligible overlap between wild-type and heterozygous RBCs (*15*). Yet heterozygous RBCs showed normal survival in wild-type mice. Although this result argues against a gradual removal of CD47 as the mechanism regulating RBC life-span, it remains possible that control of CD47 expression might be used elsewhere as a means to regulate cell fate or cell-cell interactions.

It is unclear at what level of RBC CD47 expression the negative signal is sufficiently attenuated to allow phagocytosis. Rh polypeptides are expressed as a complex with CD47 on the cell surface. Rh_{null} individuals fail to express Rh antigen–bearing polypeptides on their RBCs (*28*), and consequently they express CD47 at ≤25% of normal levels. In contrast, CD47 levels are normal on Rhnull leukocytes and presumably also on splenic macrophages of Rh_{null} individuals. Rh_{null} individuals have hemolytic anemia, reticulocytosis, and stomatocytosis—all of which can be corrected by splenectomy (*28*). This parallels our transfusion model in which RBCs with reduced levels of CD47 are cleared in an environment of CD47^{+} cells. It is tempting to speculate that the elimination of Rh_{null} RBCs is secondary to reduced CD47-SIRPα signaling to splenic macrophages.

Although CD47$^{-/-}$ RBCs are recognized and eliminated in wild-type recipients, they survive normally in CD47-deficient mice. This suggests that the macrophage is regulated by the expression of CD47 on its surface or in its environment. This adaptation does not appear to be at the level of inhibitory receptor expression, because the level of SIRPα is virtually identical on CD47$^{-/-}$ and wild-type macrophages (*29*).

The data presented here demonstrate that CD47 is a crucial marker of self on RBCs. Preliminary data suggest that this is also true for other cells, such as lymphocytes (*29*). Red pulp macrophages specifically bind to circulating cells, and only CD47 expression prevents their elimination. Thus, splenic macrophages do not have to rely on activating receptors alone to differentiate between self and foreign, but can use the presence or absence of CD47 to make that distinction. Ovarian cancer cells express high levels of CD47 (*13*, *30*), and CD47 analogs are encoded by smallpox and vaccinia viruses (*11*–*13*). In both of these instances, it is possible that the pathogen is taking advantage of SIRPα signaling to disable normal defenses. Similarly, down-regulation of SIRPα might confer selective advantages to malignancies of myeloid origin (*31*).

References and Notes

1. L. L. Lanier, *Annu. Rev. Immunol.* **16**, 359 (1998).
2. W. M. Yokoyama, *Curr. Biol.* **7**, 110 (1995).
3. H. G. Ljunggren and K. Kärre, *J. Exp. Med.* **162**, 1745 (1985).
4. E. O. Long, *Annu. Rev. Immunol.* **17**, 875 (1999).
5. P. Höglund *et al.*, *Eur. J. Immunol.* **28**, 370 (1998).
6. J. Samaridis and M. Colonna, *Eur. J. Immunol.* **27**, 660 (1997).
7. M. Colonna, F. Navarro, M. López-Botet, *Curr. Top. Microbiol. Immunol.* **244**, 115 (1999).
8. A. Kharitonenkov *et al*, *Nature* **386**, 181 (1997).
9. P. Jiang, C. F. Lagenaur, V. Narayanan, *J. Biol. Chem.* **274**, 559 (1999).
10. E. J. Brown, L. Hooper, T. Ho, H. D. Gresham, *J. Cell Biol.* **111**, 2785 (1990).
11. F. P. Lindberg, H. D. Gresham, E. Schwarz, E. J. Brown, *J. Cell Biol.* **123**, 485 (1993).
12. F. P. Lindberg *et al*, *J. Biol. Chem.* **269**, 1567 (1994).
13. I. G. Campbell, P. S. Freemont, W. Foulkes, J. Trowsdale, *Cancer Res.* **52**, 5416 (1992).
14. W. J. Mawby, C. H. Holmes, D. J. Anstee, F. A. Spring, M. J. Tanner, *Biochem. J.* **304**, 525 (1994).
15. F. P. Lindberg *et al*, *Science* **274**, 795 (1996).
16. Male and female CD47$^{-/-}$ C57BL/6J mice, backcrossed to C57BL/6J (Jackson Laboratory) for 16 or more generations, and their heterozygous and homozygous littermates were from our breeding colony. All experiments described were also reproduced with isogenic 129sv/eg mice with very similar results (not shown). Rag1$^{-/-}$ mice (*32*) on a C57BL/6J background were a gift from D. Chaplin (Washington University, St. Louis, MO). C3$^{-/-}$ mice (*33*) on a mixed 129/C56BL/6 background were a gift from H. Molina (Washington University, St. Louis, MO). Animals were kept in accordance with NIH and local guidelines and maintained in a specific pathogen-free barrier facility.
17. RBCs were stained with the fluorescent dyes 5/6-carboxyfluorescein diacetate succimidyl ester (CFSE; Molecular Probes, Eugene, OR) or PKH-26 (Sigma) and resuspended in sterile pyrogen-free 0.9% NaCl to 30% (v/v). Recipients were given 200 μl of the stained RBCs, and the clearance of fluorescent RBCs was measured by flow cytometry (Epics XL; Coulter, Hialeah, FL) of 5-μl blood samples collected from a tail vein at the time points indicated. The fraction of fluorescent RBCs of the total number of recipient RBCs studied (100,000 per sample) was determined. Levels at 5, 15, and 30 min were virtually identical. The data were normalized to the fraction at 30 min

after injection (donor RBCs constituted 4 to 6% of the total number of RBCs at this time point). Results were independent of the dye used. Control experiments with unlabeled CD47$^{-/-}$ RBCs in wild-type recipients and wild-type RBCs in CD47$^{-/-}$ recipients (detection by staining for CD47 and flow cytometry) gave similar results.
18. N. van Rooijen and A. Sanders, *J. Immunol. Methods* **174**, 83 (1994).
19. N. van Rooijen, N. Kors, G. Kraal, *J. Leukocyte Biol.* **45**, 97 (1989).
20. Dichloromethylene diphosphonate (clodronate; a gift from Roche Diagnostics/Boehringer Mannheim GmbH) liposomes was prepared as described (*18*). Clodronate (200 μl) or NaCl liposomes were given to recipient mice by tail-vein injection at 48 and 24 hours before RBC transfer. Immunohistochemical analyses revealed a complete macrophage depletion in recipient spleens 48 hours after a single injection of clodronate liposomes.
21. Spleen specimens were taken from recipients at 20 hours after the administration of PKH26-stained CD47$^{-/-}$ RBCs. Spleens were embedded in O.C.T compound (Sakura Finetek U.S.A., Torrance, CA), frozen in liquid nitrogen, and stored at −80°C. Cryostat sections (8 μm) were incubated with antibodies to F4/80 [red pulp macrophages (*34*)] or MOMA-1 [marginal metallophilic macrophages (*35*)]. After incubation with horseradish peroxidase (HRP)–conjugated secondary antibodies, F4/80^{+} and MOMA-1^{+} cells were visualized with Tyramide Signal Amplification (NEN Life Science Products, Boston, MA).
22. Y. Fujioka *et al*, *Mol. Cell. Biol.* **16**, 6887 (1996).
23. S. Adams *et al*, *J. Immunol.* **161**, 1853 (1998).
24. Wild-type spleens were digested with collagenase D (Roche Diagnostics, Indianapolis, IN) [400 U/ml in Hanks balanced salt solution (HBSS) without Ca^{2+} or Mg^{2+}] for 30 min at 37°C. After RBC lysis and extensive washing, the cells were resuspended to 5 × 10^7/ml in ice-cold HBSS with 1 mM Ca^{2+}, 1 mM Mg^{2+}, 1% human serum albumin (HSA). Macrophages were allowed to adhere for 60 min at 37°C in plastic eight-well Lab-Tek chamber slides (200 μl/well; Nalgene Nunc International, Naperville, IL). Anti-SIRPα P84 (5 μg) (*9*) or the isotype-matched control (anti-murine CD14; clone rmC5-3; Pharmingen) or no antibody was present during the last 15 min. Subsequently, 50 μl of PKH26-labeled wild-type or CD47$^{-/-}$ RBCs were added to each well for another 60 min. Nonadherent cells were washed off with warm phosphate-buffered saline (PBS)−0.1% HSA, and noningested RBCs were lysed with ACK lysis buffer. Phagocytosis index (the number of RBCs phagocytosed per 100 adherent macrophages) was determined by fluorescence microscopy (Zeiss Axioscope).
25. A. Veillette, E. Thibaudeau, S. Latour, *J. Biol. Chem.* **273**, 22719 (1998).
26. W. H. Fridman, P. Bruhns, O. Malbec, M. Daëron, *J. Biol. Chem.* **274**, 32493 (1999).
27. Bone marrow–derived macrophages were prepared as described (*36*). Mature macrophages (1.5 × 10^6) were plated on 60-mm bacteriological plastic Petri dishes (Valmark; Midwest Scientific, St. Louis, MO) for 16 hours before experiments. The cells were rinsed once with PBS, and 2 ml of cold, serum-free Iscove's modified DMEM (IMDM) was added to each dish. After 2 min at 4°C, 2 × 10^6 wild-type or CD47$^{-/-}$ RBCs were added, then allowed to settle for 3 min at 4°C, after which sodium pervanadate (Sigma) was added to 2 mM and cells were transferred to a water bath at 37°C. At the times indicated, the medium was quickly aspirated, and cells were lysed in cold lysis buffer [50 mM tris-HCl (pH 7.5), 150 mM NaCl, 1% NP-40 (Pierce, Rockford, IL), 1 mM diisopropyl, aprotinin (10 μg/ml), 2 mM sodium pervanadate]. Lysates were cleared by centrifugation and incubated for 2 hours at 4°C with anti-SIRP monoclonal antibody (mAb) P84 bound to 20 μl of goat anti-rat Sepharose (ICN, Costa Mesa, CA) for 2 hours at 4°C. After two washes in lysis buffer, immunoprecipitated proteins were eluted with reducing SDS–polyacrylamide gel electrophoresis (PAGE) sample buffer, separated on 8% SDS-PAGE, and transferred to a polyvinylidene difluoride membrane (Millipore, Bedford, MA). Tyrosine phosphorylation was detected by Western blot with anti-phosphotyrosine mAb 4G10, followed by HRP-conjugated secondary antibody and enhanced chemoluminescence as described (*36*).
28. Reviewed in N. D. Avent and M. E. Reid, *Blood* **95**, 375 (2000).
29. F. P. Lindberg *et al.*, unpublished data.
30. L. G. Poels *et al.*, *J. Natl. Cancer Inst.* **76**, 781 (1986).
31. M. Seiffert *et al*, *Blood* **94**, 3633 (1999).
32. P. Mombaerts *et al.*, *Cell* **68**, 869 (1992).
33. M. R. Wessels *et al.*, *Proc. Natl. Acad. Sci. U.S.A.* **92**, 11490 (1995).
34. M. D. Witmer and R. M. Steinman, *Am. J. Anat.* **170**, 465 (1984).
35. G. Kraal and M. Janse, *Immunology* **58**, 665 (1986).
36. T. Roach *et al.*, *Curr. Biol.* **7**, 408 (1997).
37. We thank T. Steinberg, W. Yokoyama, J. Atkinson, and E. Brown for critically reading the manuscript; D. Chaplin, H. Molina, and P. Leenen for reagents; and E. Ford for technical assistance. Supported by grants from the NIH (GM57573-01), the American Diabetes Association, the Washington University–Monsanto Research Agreement, a pilot grant from the Howard Hughes Medical Institute, and the Medical Research Service of the Depatment of Veterans Affairs. P.-A.O is supported by a postdoctoral fellowship from the Umeå University–Washington University exchange program and by the Swedish Medical Research Council.

15 February 2000; accepted 25 April 2000

Selectivity for 3D Shape That Reveals Distinct Areas Within Macaque Inferior Temporal Cortex

Peter Janssen, Rufin Vogels,* Guy A. Orban

The anterior part of the macaque inferior temporal cortex, area TE, occupies a large portion of the temporal lobe and is critical for object recognition. Thus far, no relation between anatomical subdivisions of TE and neuronal selectivity has been described. Here, we present evidence that neurons selective for three-dimensional (3D) shape are concentrated in the lower bank of the superior temporal sulcus, whereas neurons in lateral TE are generally unselective for 3D shape, though equally selective for 2D shape. These findings reveal that TE consists of at least two distinct areas, one of which processes a specific object property.

The inferior temporal cortex (IT) is part of the ventral visual stream, which is known to be critical for object recognition (*1, 2*). Neurons in the anterior part of IT, area TE (Fig. 1), respond selectively to object attributes (*3*). For over three decades, researchers have been puzzled by the organization of this large cortical region [up to 380 mm^2 (*4*)]. Although TE can be divided into a number of subregions on the basis of anatomical criteria (*5*), no clear link between the anatomy and neuronal selectivity has yet emerged. Here, we present evidence, based on 3D shape–selectivity, that at least two areas can be distinguished within TE: the lower bank of the superior temporal sulcus (STS) and lateral TE.

Thirty-two pairs of disparity-defined (*6*) curved 3D shapes served as stimuli. The 3D shape–selectivity was assessed by comparing the responses of single TE neurons to the members of pairs of 3D shapes differing only in the sign of their binocular disparity (concave versus convex) (*7*). Reconstruction of the position of each recorded neuron (Fig. 1) (*8*) showed that 142 neurons were recorded in the lower bank of the STS and 82 in lateral TE (*9*). Figure 2A illustrates the responses of an STS neuron that responded strongly to the concave, but not to the convex shape (*10*). Monocular presentations to left or right eye separately evoked only minimal responses (*11*). This 3D shape–selective response contrasted markedly with the responses of lateral TE neurons. Although the lateral TE neuron of Fig. 2B responded to the concave shape, the response to the convex shape was equally strong. Moreover, the monocular presentations elicited responses that were similar to those in the stereo conditions. This response pattern, combined with the 2D shape–selectivity revealed by the search test (*7*), indicates that this neuron was not sensitive to 3D structure, but simply responded to the 2D shape.

Overall, 56% of the tested STS neurons were selective for 3D shape, compared to only 12% in lateral TE ($\chi^2 = 40.9$, $P < 0.001$) (*12, 13*). Moreover, the degree of 3D selectivity was much lower in lateral TE (*14*), though the mean net response to the preferred 3D shape did not differ significantly between the two subdivisions (20.2 and 19.1 spikes per second for the STS and lateral TE, re-

Laboratorium voor Neuro-en Psychofysiologie, Medical School, Katholieke Universiteit Leuven, Leuven B-3000, Belgium.

*To whom correspondence should be addressed. E-mail: Rufin.Vogels@med.kuleuven.ac.be